Applied Geochemistry 23 (2008) 3143–3154

Contents lists available at ScienceDirect

Applied Geochemistry

journal homepage: www.elsevier.com/locate/apgeochem

Geochemical processes underlying a sharp contrast in groundwater arsenic concentrations in a village on the Red River delta, Vietnam

Elisabeth Eiche [a,*], Thomas Neumann [a], Michael Berg [b], Beth Weinman [c], Alexander van Geen [d], Stefan Norra [a], Zsolt Berner [a], Pham Thi Kim Trang [e], Pham Hung Viet [e], Doris Stüben [a]

[a] *Institute of Mineralogy and Geochemistry, Universität Karlsruhe (TH), 76131 Karlsruhe, Germany*
[b] *Eawag, Swiss Federal Institute of Aquatic Science and Technology, 8600 Dübendorf, Switzerland*
[c] *Earth and Environmental Sciences, Vanderbilt University, Nashville, TN 37240, USA*
[d] *Lamont-Doherty Earth Observatory of Columbia University, Palisades, NY 10964, USA*
[e] *Centre for Environmental Technology and Sustainable Development (CETASD), Hanoi University of Science, Hanoi, Viet Nam*

ARTICLE INFO

Article history:
Available online 11 July 2008

ABSTRACT

The spatial variability of As concentrations in aquifers of the Red River Delta, Vietnam, was studied in the vicinity of Hanoi. Two sites, only 700 m apart but with very different As concentrations in groundwater (site L: <10 μg/L vs. site H: 170–600 μg/L) in the 20–50 m depth range, were characterized with respect to sediment geochemistry and mineralogy as well as hydrochemistry. Sequential extractions of the sediment were carried out in order to understand why As is released to groundwater at one site and not the other. No major differences were observed in the bulk mineralogy and geochemistry of the sediment, with the exception of the redox state of Fe oxyhydroxides inferred from sediment colour and diffuse spectral reflectance. At site H most of the As in the sediment was adsorbed to grey sands of mixed Fe(II/III) valence whereas at site L As was more strongly bound to orange-brown Fe(III) oxides. Higher dissolved Fe and low dissolved S concentrations in groundwater at site H (~14 mg Fe/L, <0.3 mg S/L) suggest more strongly reducing conditions compared to site L (1–2 mg Fe/L, <3.8 mg S/L). High concentrations of NH_4^+ (~10 mg/L), HCO_3^- (500 mg/L) and dissolved P (600 mg/L), in addition to elevated As at site H are consistent with a release coupled to microbially induced reductive dissolution of Fe oxyhydroxides. Other processes such as precipitation of siderite and vivianite, which are strongly supersaturated at site H, or the formation of amorphous Fe(II)/As(III) phases and Fe sulfides, may also influence the partitioning of As between groundwater and aquifer sands.

The origin of the redox contrast between the two sites is presently unclear. Peat was observed at site L, but it was embedded within a thick clayey silt layer. At site H, instead, organic rich layers were only separated from the underlying aquifer by thin silt layers. Leaching of organic matter from this source could cause reducing conditions and therefore potentially be related to particularly high concentrations of dissolved NH_4^+, HCO_3^-, P and DOC in the portion of the aquifer where groundwater As concentrations are also elevated.

1. Introduction

The enrichment of natural waters with As from geogenic sources poses a severe health problem throughout the world. Cases of arsenicosis have long ago been attributed to elevated As levels in drinking water in countries such as Taiwan (Tseng et al., 1968), Chile (Zaldivar, 1974), Mexico (Del Razo et al., 1990) and Argentina (Nicolli et al., 1989). However, the international scientific community was truly mobilized only after the discovery of elevated groundwater As concentrations throughout the densely

---

* Corresponding author. Fax: +49 721 608 4170.
E-mail address: elisabeth.eiche@img.uni-karlsruhe.de (E. Eiche).

0883-2927/$ - see front matter © 2008 Elsevier Ltd. All rights reserved.
doi:10.1016/j.apgeochem.2008.06.023

populated Bengal Basin, which includes Bangladesh and the state of West Bengal in India (Das et al., 1996). Other regions with elevated As levels in groundwater have since been identified, primarily in relatively young alluvial deposits, such as the densely populated deltas of the Mekong and Red River in Cambodia and Vietnam (Berg et al., 2001, 2007; Polya et al., 2005; Buschmann et al., 2007, 2008; Larson et al., 2008; Rowland et al., 2008; Winkel et al., 2008a).

Over the years, various processes have been postulated in order to explain high As concentrations in groundwater. The reductive dissolution of different Fe oxides, which are common in sedimentary environments, is widely accepted as a key process for the release of As into groundwater (Nickson et al., 2000; Dowling et al., 2002; Harvey et al., 2002; Stüben et al., 2003; Charlet and Polya, 2006). However, the reduction of Fe oxides alone cannot explain the wide range of groundwater As concentrations encountered in similarly reducing aquifers (Polizzotto et al., 2006; Stute et al., 2007; van Geen et al., 2008a). What is clear is that the microbially driven decomposition of organic matter plays an important role for the onset and the maintenance of reducing conditions in aquifers (Lovley, 1992; Lovley and Chapelle, 1995; Rowland et al., 2006, 2007). Despite its importance, not enough is known about the nature and the origin of this organic matter (Rowland et al., 2006). Different sources have been proposed over the years, including peat layers or confining sediment layers rich in total organic carbon (TOC) (Lovley and Chapelle, 1995; McAthur et al., 2001; Zheng et al., 2004; Winkel et al., 2008b, 2008a), recharge from ponds and rivers commonly high in dissolved organic carbon (DOC), as well as anthropogenic sources of organic matter (Bukau et al., 2000; McAthur et al., 2001; Harvey et al., 2002). Further processes under discussion which could influence the As concentration in groundwater are competition with other dissolved ions like PO_4^{3-} (Su and Pulse, 2001) or HCO_3^- (Harvey et al., 2002; Apello et al., 2002), oxidation of pyrite (Chowdhury et al., 1999) or precipitation and dissolution of secondary mineral phases (e.g. siderite, magnetite, amorphous phases incorporating As) (Sengupta et al., 2004; Swartz et al., 2004; Herbel and Fendorf, 2006). Polizzotto et al. (2006) have also suggested that As released in the surface soil by redox cycling could be transported downwards towards the sandy aquifer.

There is still much disagreement about causes underlying the patchy As distribution commonly observed in affected areas. Pronounced differences in As levels can be found within distances of 100 m (BGS/DPHE, 2001; van Geen et al., 2003; McAthur et al., 2004). Recent studies in portions of the Red River Delta have also revealed significant differences even within short distances of 10–20 m (Berg et al., 2007). Several explanations have been proposed for the complex spatial distribution of As, including differences in the subsurface lithology, mineralogy, geochemistry, local hydrology and the abundance of organic material (Pal et al., 2002; van Geen et al., 2006; Stute et al., 2007). Considerable uncertainty remains, however, and too little is known to predict with confidence how As concentrations will evolve over time and to what extent aquifers currently providing potable water can be relied on in the future (Zheng et al., 2005).

In an attempt to address some of these unresolved issues, the village of Van Phuc in northern Vietnam was selected for detailed investigations. In this village the spatial As distribution is known to be highly variable (Berg et al., 2008). Here geochemical results from two sediment cores recovered from two contrasting environments are presented and discussed, as well as profiles of groundwater properties obtained from nests of wells installed at the same two locations.

2. Study area

Van Phuc village is located in the Red River delta (Bac Bo Plain, RRD), 10 km SE of Hanoi (Fig. 1). The delta covers an area of 11,000 km^2 and is used mainly for agriculture by a population of about 11 million (Berg et al., 2001). The morphology of the delta has been controlled by the highly variable discharge of the Red River over the past millennia. Throughout this period, riverbed movement has caused erosion as well as accumulation of alluvial material. In addition, a succession of transgressions and regressions linked to climate fluctuations has contributed sediment of marine origin. Due to the multitude of sedimentation processes occurring in the RRD, the lithology of the delta sediments is highly complex and sediment sequences vary considerably within short distances (Mathers and Zalasiewicz, 1999; Tanabe et al., 2006).

Holocene as well as Pleistocene sediments are present in the larger Hanoi area (Trafford et al., 1996). Southwest of Hanoi the Holocene sediments contain high amounts of natural organic matter (NOM). The Pleistocene and Holocene aquifers along the Red River are mainly recharged by water from the river itself, at least in part because of the large withdrawals supplying the city of Hanoi (Berg et al., 2007, 2008).

Van Phuc village is located between the Red River and a levee that protects the south-western parts of Hanoi from annual flooding (Fig. 1). The village itself is occasionally flooded for a few days during the rainy season. The aquifer consists of faintly bedded Holocene and Pleistocene sediments up to depths >40 m (Berg et al., 2007). The land is mainly used for agriculture (corn, medicinal plants, cabbage). Most of the fields are irrigated during the dry season either by water from ponds or, to a lesser extent, by groundwater from dug wells. However, there are no rice paddies in the region of Van Phuc.

Groundwater is the main source of drinking water in Van Phuc. Households commonly pass raw groundwater through sand filters which lowers As concentrations on average by 80% due to co-precipitation with Fe (Berg et al., 2006). Between the rainy and dry season, the depth of the water table varies widely in both the aquifer ($\leqslant$4 m) and in the Red River (7–10 m). The similar major ion composition of groundwater in Van Phuc and water from the Red River is consistent with a significant component of recharge originating from the river, as recently documented at different locations upstream (Postma et al., 2007; Berg et al., 2008).

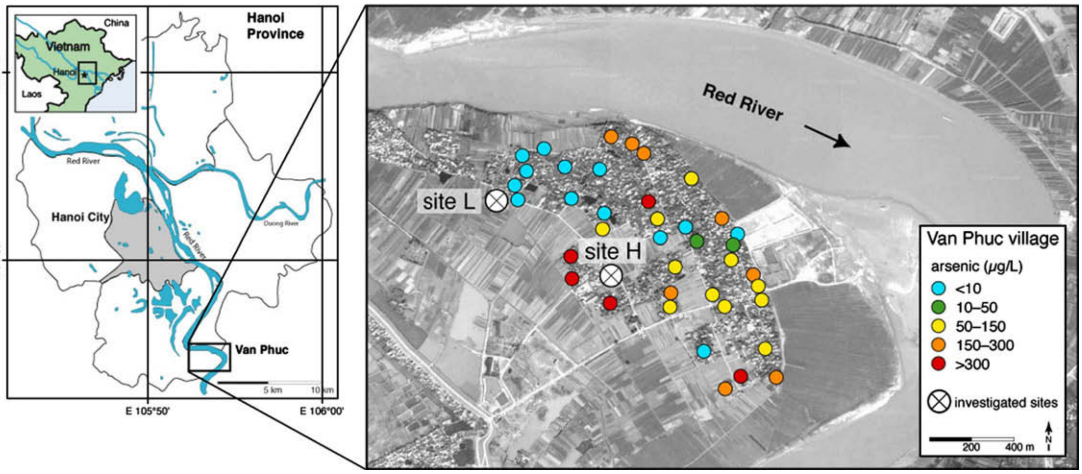

Fig. 1. Map depicting the study sites in Van Phuc village situated some 10 km south of the centre of Hanoi city (modified map from Berg et al., 2007). Arsenic in groundwater shows a patchy distribution in this village. Site L (low) has particularly low levels of dissolved As (3 ± 2 µg/L), whereas site H (high) features very high-As concentrations (400 ± 135 µg/L). The two sites are 700 m apart from each other. The satellite image was taken from google-earth (earth.google.com).

In April 2006, two ~55 m-long sediment cores were recovered by rotary drilling at site L, located in the low-As area, and at site H in the high-As area (Fig. 1). The distance between the two sites is only 700 m. Nine monitoring wells ranging from 17 to 55 m in depth and consisting of PVC casings with a 1-m long sand trap at the bottom were also installed at each site (Fig. 2). To avoid infiltration of surface water, concrete pads surrounding the upper

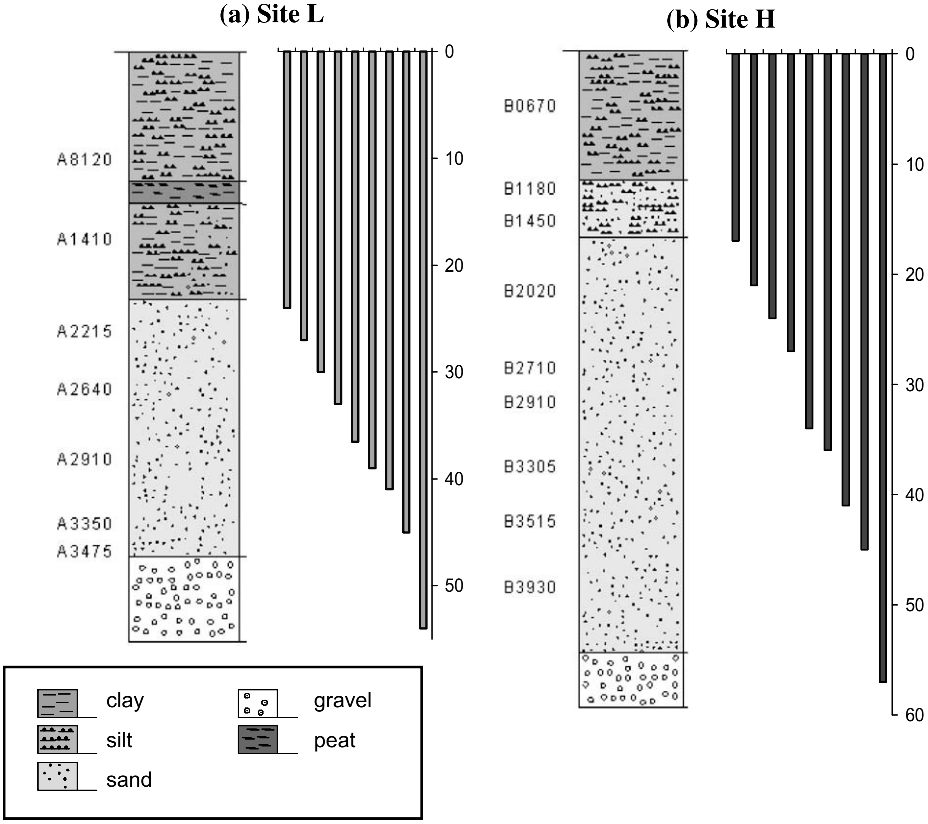

Fig. 2. Lithological logs of the boreholes drilled in April 2006 at (a) site L and (b) site H. Each site was equipped with a nest of nine monitoring wells. The labelling on the left side of each log marks the samples taken for the sequential extraction procedure.

steel casing were installed and each well was capped with a steel screw cap.

3. Materials and methods

3.1. Water sampling and analysis

Water samples were taken from the nine monitoring wells at each site. Prior to sampling, groundwater was pumped for about 10 min with an electrical pump to avoid any contamination by stale water. Portable YSI 556 and WTW Multi 340i (John Morris Scientific Pty Ltd.) systems were used to measure Eh, pH, temperature, conductivity and O_2. Disposable cartridges that selectively adsorb As(V) were used in the field to determine the speciation of As (Meng et al., 2001) by difference relative to total dissolved As concentrations. For analysis of metals, NH_4^+ and total P (P_{tot}), groundwater samples were filtered on-site (cellulose nitrate filter, 0.45 μm) and acidified with HNO_3 (65%, Fluka, Switzerland) to a pH < 2. For anions, alkalinity ($\sim HCO_3^-$) and dissolved organic C (DOC), the samples were left unfiltered and non-acidified. Pre-rinsed polypropylene bottles were filled with the samples, sealed tightly and stored in the dark at 4 °C until analysis. For alkalinity the samples were filtered in the laboratory before analysis. In order to check the quality of the alkalinity analysis in the laboratory, control-measurements were done in the field with a test kit (Merck, Germany). The results of laboratory and field measurements were within 10% and therefore a significant alteration of the alkalinity during storage and transport can be excluded.

Dissolved As, P_{tot} and S concentrations were measured by high-resolution ICP-MS (Element 2, Thermo Fisher, Bremen, Germany). The analysis of Fe, Mn, Ca, Mg and Ba was conducted by ICP-OES (Spectro Ciros CCD, Kleve, Germany). Ammonium was analysed by photometry; NO_3^- and Cl^- by ion chromatography (Dionex, Switzerland), alkalinity by titration and DOC by means of a TOC 5000 Analyser (Shimadzu, Switzerland). All groundwater analyses were carried out at Eawag. The quality of the results can be taken as reasonably good as the ion balance varies within less than 10%.

3.2. Sediment sampling and analysis

Samples were taken from the sediment cores in intervals of 1-m and more frequently in cases of significant changes in colour, grain size or texture. About 100 g of fresh sediment material was placed in polypropylene bags and later flushed with N_2 to minimize oxidation processes in the time between sampling and analysis. Before transport the samples were packed into Mylar bags and flushed again with N_2. The samples were sent to Germany where they were frozen until further analysis.

Prior to analysis, subsamples of the sediment were dried at 40 °C and ground to powder. The elemental composition of the sediments was determined by energy dispersive X-ray fluorescence analysis (Spectra 5000, Atomica). Precision (better than 5%) was calculated from repeated measurements of a standard material, whereas accuracy (better than 10%) was checked by including different reference materials, e.g. GXR 2 (Park City, Utah, USA). Total S and C contents were quantified by a Carbon–Sulphur-Analyser (CSA 5003, Leybold Heraeus, Germany), and inorganic C was determined by Carbon–Water-Analysis (CWA 5003, Leybold Heraeus, Germany). The organic C content was calculated by subtracting inorganic C from total C. The mineral composition of the sediment samples was determined by means of X-ray diffraction (XRD) analysis (Kristalloflex D500, Siemens, Germany) at 40 kV and 25 mA. CuKα1-radiation was used at angles between 3° and 63°. The semi-quantitative evaluation of the spectra was based on calibration curves obtained from different samples with known mineral composition (Snyder and Bish, 1989).

The grain size distribution of the sediment was measured at Vanderbilt University using a laser-granulometer (Mastersizer 2000, Malvern). The grain sizes were grouped as follows: clay: <2 μm, silt: 2–63 μm, sand: >63 μm.

A CM2005d spectrophotometer (Minolta Corp., USA) was used in order to measure the diffuse reflectance spectrum of freshly collected sediment in the field relative to a white standard plate consisting of $BaSO_4$. Each measurement was repeated three times. The difference in reflectance between 530 and 520 nm was calculated from the measurements in order to obtain a value (ΔR in % reflectance) that previous work has shown is inversely related to the Fe(II)/Fe ratio in the acid-leachable fraction of aquifer particles in Bangladesh (Horneman et al., 2004).

For sequential extractions of sediment from 7 intervals at site L and 9 at site H (Fig. 2), 0.5 g of fresh sediment was weighed into centrifuge tubes and the appropriate amount of leaching solution was added. After each step the solutions were centrifuged at 4500 rpm for 15 min and then decanted. The solutions were kept in a refrigerator until further measurements by (HR-) ICP-MS (Axiom, VG Elemental). The procedure of Keon et al. (2001) was slightly modified (Table 1). In order to avoid interferences with ICP-MS measurements, 0.05 M $(NH_4)_2SO_4$ (Wenzel et al., 2001) was used instead of $MgCl_2$ in the first step. Furthermore, in step 5 the application of Ti–citrate–EDTA was changed to dithionite–citrate–bicarbonate (DCB) solution described in van Herreweghe et al. (2003). Finally, steps 7 and 8 of the original procedure were combined into one step. Specific conditions and the phases targeted by each step are listed in Table 1. In order to check the reproducibility of the sequential extraction, one subsample was first homogenized and afterwards separated into 3 aliquots. In 5 out of 7 of the fractions the results for Fe and As concentrations did not differ by more than 10%, which constitutes a reasonable level of reproducibility.

3.3. Geochemical modelling and statistical analysis

The saturation indices of different minerals like calcite, dolomite, siderite etc. were calculated on the basis of the hydrochemical results with the PHREEQC-program (Parkhurst and Appelo, 1999). Statistical analysis of water as well as sediment data was done using the STATISTICA – program (StatSoft, USA, Version 6). The p-value for the given correlations is always <0.01.

Table 1
Sequential extraction scheme used for the sediment leaching

Step	Target phase	Extractant	Conditions	Ref.
F1	Ionically bound	0.05 M $(NH_4)_2SO_4$	25 mL, 4 h, 25 °C, one repetition, one water wash	[1]
F2	Strongly adsorbed	0.5 M NaH_2PO_4	40 mL, 16 h and 24 h, 25 °C, pH 5, one repetition of each time duration, one water wash	[2]
F3	Co-precipitated with acid volatile sulfides, carbonates, Mn-oxides, very amorphous Fe oxides	1 M HCl	40 mL, 1 h, 25 °C, one repetition, one water wash	[2]
F4	Co-precipitated with amorphous Fe oxides	0.2 M NH_4^+-oxalate/oxalic acid	40 mL, 2 h, 25 °C, pH 3, dark (wrapped in Al-foil), one repetition, one water wash	[2]
F5	Co-precipitated with crystalline Fe oxyhydroxides	DCB: 0.5 M Na-citrate + 1 M $NaHCO_3$; 0.5 g $Na_2S_2O_4 \times H_2O$	35 mL Na-citrate + 2.5 mL $NaHCO_3$ (heating to 85 °C), addition of 0.5 g $Na_2S_2O_4 \times H_2O$, 15 min at 85 °C, one repetition, one water wash	[3]
F6	Co-precipitated with silicate	10 M HF; 5 g boric acid	40 mL, 1 h and 24 h, 25 °C, one repetition of each time step, after 16 h, addition of boric acid, one hot wash	[2]
F7	As-sulphides, co-precipitated with sulphides, organic matter	16 M HNO_3; 30% H_2O_2	Method according to EPA 3050B	

[1] Wenzel et al. (2001), [2] Keon et al. (2001), [3] van Herreweghe et al. (2003).

4. Results and interpretation

4.1. Lithology and reflectance

Based on grain-size, the core at site L can be separated into 3 distinct layers: a silty (75 ± 12%) layer extending from the top to a depth of 23 m, a sandy (65 ± 16%) intermediate layer with varying amounts of silt to a depth of 48 m, and a coarse gravel layer extending to a depth of 54 m where drilling stopped (Fig. 3a). Noteworthy are two distinct black, organic rich intervals at depths of ~11 m and ~13 m, respectively, within the upper silty layer. This layer is an aquitard, based on the low hydrologic conductivity (K: $\sim 7 \times 10^{-8}$ m/s) estimated from the grain size distribution (Beyer, 1964). The transition to the underlying aquifer at a depth of 23 m is marked by a Fe-concretion consisting of goethite and quartz. The aquifer is separated into an upper sand (K: $\sim 2 \times 10^{-6}$ m/s) and a lower gravel deposit (Fig. 3a). The upper part is ~25 m thick and mainly composed of fine to medium sands interspersed with silty layers, mostly brown to yellowish-brown in colour.

The lithology of core H differs significantly from core L and is more heterogeneous (Fig. 3b). The upper silt (68 ± 20%) layer is only ~10 m thick and the colour changes from reddish-brown to greyish at ~7 m. The estimated permeability is comparable to the clayey silt at site L (K: $\sim 7 \times 10^{-8}$ m/s). Below this layer, alternating clayey silt, silty fine sands, and fine sands were observed to a depth of ~21 m. Within this layer the hydraulic conductivity increases to (K: $\sim 4 \times 10^{-6}$ m/s) until deeper in the aquifer when hydraulic conductivity increases further (K: $\sim 8 \times 10^{-6}$ m/s) due to the prevalence of sand (61 ± 20%) with varying amounts of silt. Noteworthy is a change in colour from greyish to brownish at ~44 m. At a depth of 55 m, a much coarser gravel layer appears as at site L.

The spectral reflectance data are consistent with changes in the colour of the sediment and can be related more quantitatively to changes in the redox state of acid-leachable Fe oxyhydroxides (Horneman et al., 2004). At site L, the peat layer corresponds to an interval of particularly low ΔR (<0.1) whereas values >0.7 (Fig. 3a) in the underlying aquifer are typical for oxidized orange sediments. Values of $\Delta R < 0.25$ in the grey sands at site H (Fig. 3b) are consistent with more reducing conditions throughout the 7–44 m depth range (van Geen et al., 2006). An increase in ΔR towards the bottom of the core at site H parallels the observed change in colour and indicates a transition towards less reducing conditions.

4.2. Hydrochemistry

4.2.1. Site L

The hydrochemistry is distinctly different at the two sites. As indicated by the Piper diagram in Fig. 4, the water at site L can be classified as Ca–(Na)–Mg–HCO_3 type, whereas the water at site H belongs to a Ca–HCO_3 type. Low Cl^- concentration in combination with Ca over Mg predominance is typical for deltaic groundwater (White et al., 1963; Stüben et al., 2003) and the Red River (Berg et al., 2008).

Concentrations of As in groundwater at site L range from 0.9 to 7.8 µg/L and are below the WHO-limit of 10 µg/L. Concentrations remain very low throughout the sandy aquifer, with 7.8 µg/L reached only in the gravel layer (Fig. 5). Fifty to ninty percent of As in groundwater is present as As(III) at site L. The pH (6.7 ± 0.2) is also quite constant throughout the depth profile. The absence of NO_3^- and high dissolved Mn concentrations (1.1 ± 1.1 mg/L) (Fig. 5) suggest that the groundwater at site L can be considered as Mn-reducing with regard to the classical redox sequence, at least in the upper part of the profile. However, the presence of dissolved Fe (1.8 ± 0.6 mg/L) throughout the depth range and the decrease in dissolved S to <0.4 mg/L below 30 m depth (Fig. 5) suggest some overlap with reactions typically associated with more strongly reducing conditions (sulphide and CH_4 were not measured, but the freshly pumped groundwater did not smell of H_2S). The mean molar Fe/As ratio in the water at site L is very high (>1000), although both Fe- and As-concentrations are very low. The conductivity (230 ± 64 µS/cm) points towards relatively low mineralization in the aquifer at site L, which is consistent with low concentrations of Ca (25 ± 13 mg/L), Mg (21 ± 10 mg/L) and Ba (67 ± 32 µg/L)

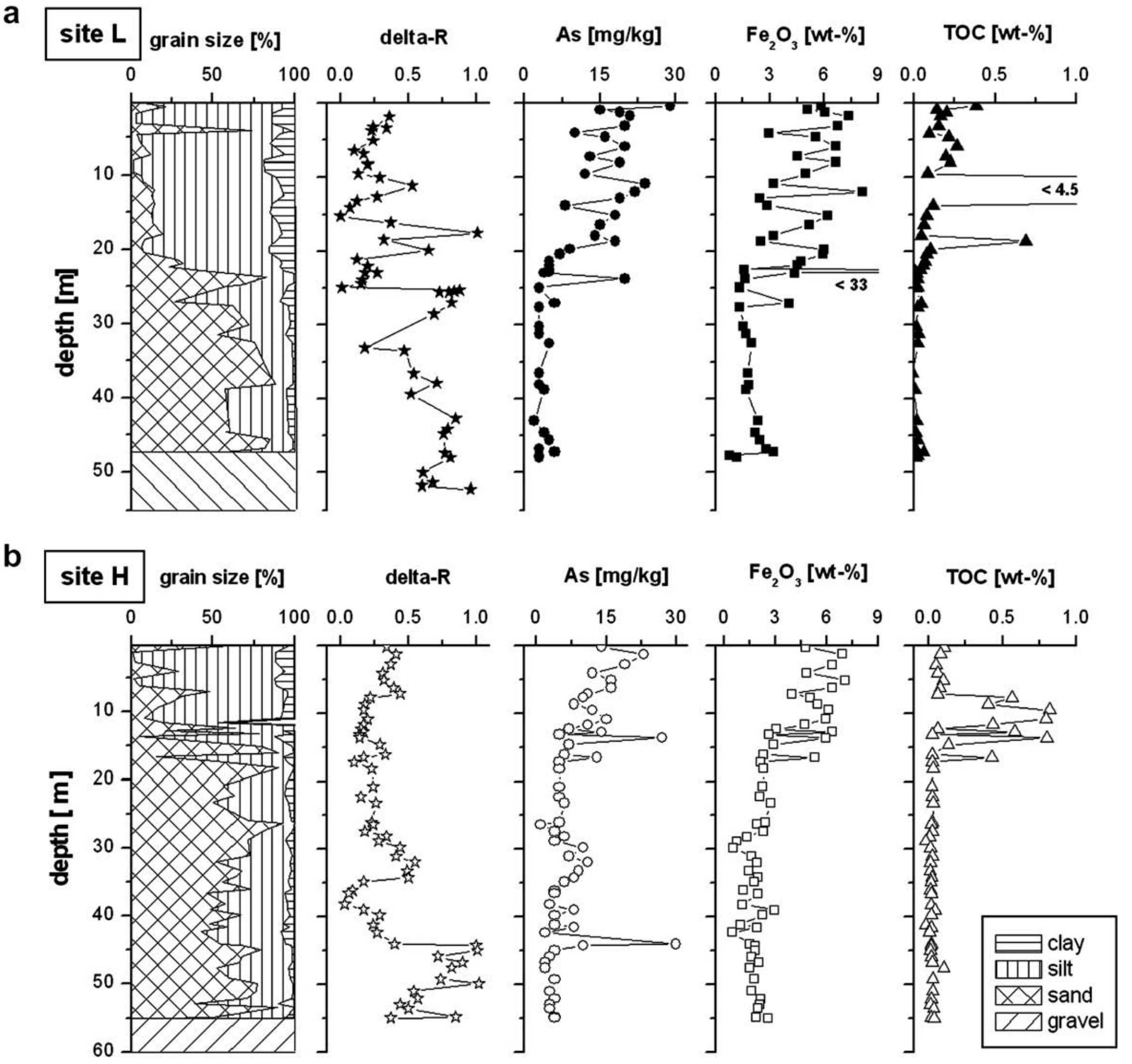

Fig. 3. Depth profiles of grain size distribution in cumulative percentage of clay (<2 μm), silt (<63 μm), sand (>63 μm) and gravel (>2 mm), reflectance (Δ*R* at 520 nm), concentration of As, Fe and TOC at site L (3a) and site H (3b).

compared to site H. Typical indicators of biodegradation such as NH_4^+ (0.2 ± 0.1 mg/L), DOC (1.3 ± 0.6 mg/L), HCO_3^- (250 ± 80 mg/L) as well as P_{tot} (70 ± 40 μg/L) are generally low in concentration (Fig. 5), suggesting limited organic turnover in the aquifer at site L. The significant correlation between the sum of Ca and Mg with HCO_3^- ($r = 0.99$, $n = 9$) suggests that these 3 ions mainly originate from the dissolution of calcite and dolomite. Calcite ($SI_{calcite} = -1 \pm 0.6$) and dolomite ($SI_{dolomite} = -1.7 \pm 1$) are subsaturated, especially in the upper part of the aquifer at site L (Fig. 6a). The corresponding molar ratio of $[HCO_3^-]/[Mg + Ca] \sim 3$ indicates, however, that sources other than carbonate dissolution contribute to the HCO_3^- in the groundwater.

4.2.2. Site H

In contrast to site L, As concentrations at site H are generally well above 10 μg/L and range from 170 to 600 μg/L in the sandy aquifer. More than 90% of As in groundwater occurs in the reduced As(III) form. The concentration of As declines sharply to 7 μg/L (Fig. 5) in groundwater pumped from the coarse gravel layer at the bottom of the section. The pH (7.1 ± 0.1) at site H is slightly higher than at site L. The groundwater is characterized by high concentrations of dissolved Fe (14.5 ± 5.6 mg/L) although dissolved Mn (0.8 ± 0.7 mg/L) levels are comparable to site L. Concentrations of NO_3^- and dissolved S are not detectable throughout at site H (Fig. 5). There is a significant correlation between dissolved Fe and Eh ($r = 0.89$, $n = 9$), suggesting reductive dissolution of Fe-minerals in the aquifer at site H. The molar Fe/As-ratio of ~100 in groundwater is comparable to Fe/As ratios reported by Berg et al. (2008) in Van Phuc and Thuong Cat for aquifers that are elevated in As. Concentrations of NH_4^+ (10 ± 7 mg/L), P_{tot} (0.6 ± 0.3 mg/L), HCO_3^- (490 ± 70 mg/L) as well as DOC (2.59 ± 1.4 mg/L) all suggest microbial degradation of organic material that is most intense in the upper part of the profile at site H and decreases in intensity with depth (Fig. 5). Higher conductivities (490 ± 40 μS/cm) measured at site H compared to

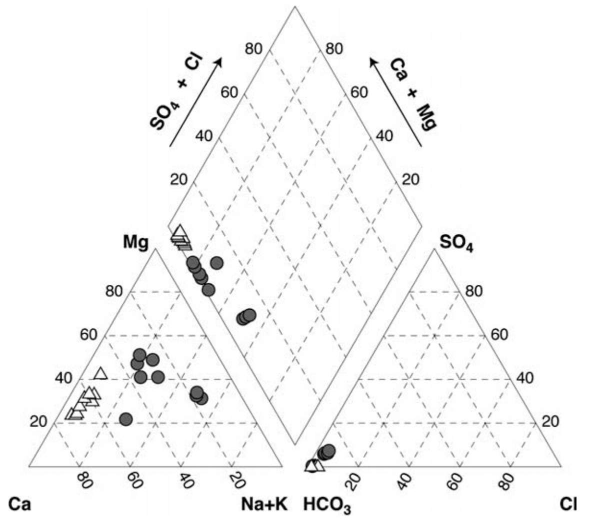

Fig. 4. Piper diagram based on the hydrochemical data at site L (●) and H (△). The groundwater can be classified as Ca–(Na)–Mg–HCO_3 type at site L, and as Ca–HCO_3 type at site H.

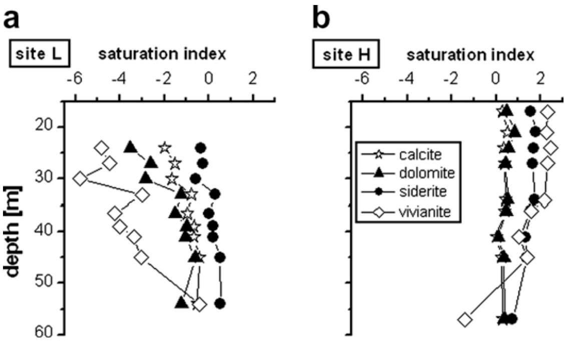

Fig. 6. Depth profiles of saturation indices of calcite, dolomite, siderite and vivianite at site L (a) and site H (b).

site L points towards enhanced mineralization, especially in the upper part of the profile (Fig. 5). Elevated concentrations of dissolved Ca (110 ± 15 mg/L) and Ba (590 ± 230 μg/L) suggest dissolution of minerals such as gypsum or barite, which are both undersaturated over the entire profile at site H (data not shown). However, the groundwater is supersaturated with respect to calcite as well as dolomite at this site (Fig. 6b). Since there is no correlation between HCO_3^- and the sum of Ca^{2+} and Mg^{2+} concentrations, elevated levels of HCO_3^- in shallow aquifers at site H are probably not the result of calcite or dolomite dissolution but, instead, the product of mineralization of NOM. This interpretation is consistent with the significant correlation between HCO_3^- and NH_4^+ ($r = 0.95$, $n = 9$) as well as DOC ($r = 0.86$, $n = 9$).

The composition of groundwater suggests the formation of new Fe phases at site H. There is a correlation be-

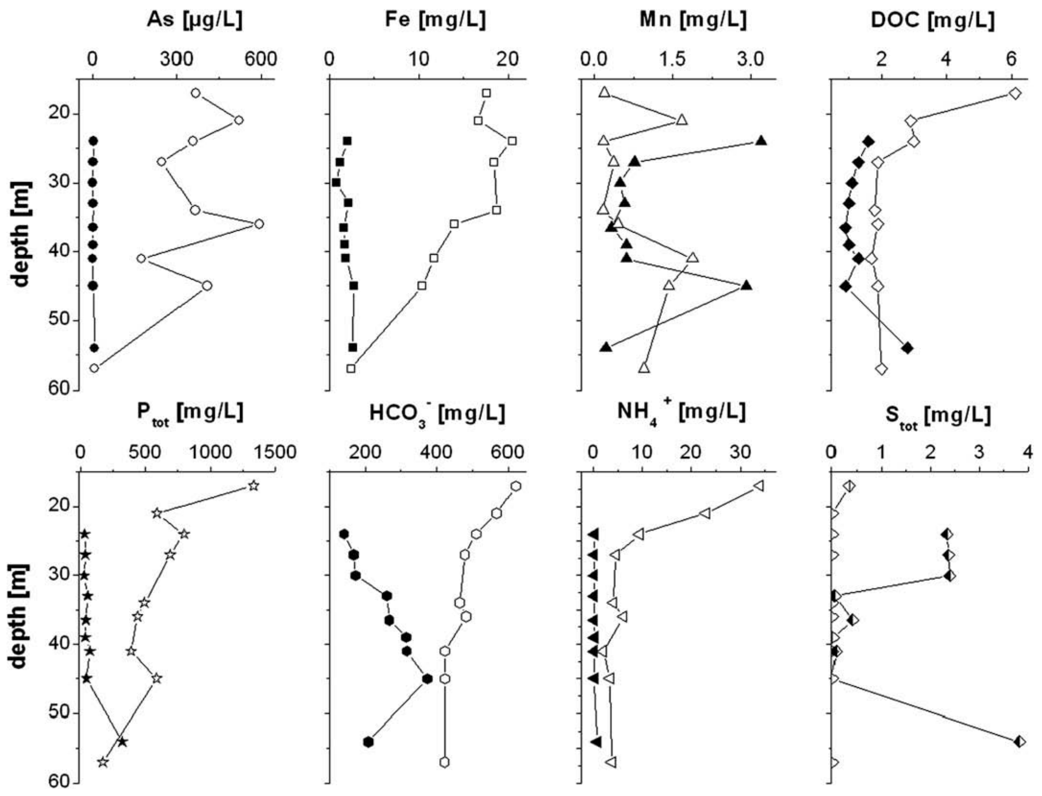

Fig. 5. Depth profiles of dissolved As, Fe, Mn, DOC, total P, HCO_3^-, NH_4^+ and total S (zero values: below detection limit of 5 μg/L) analysed in the groundwater from site L (closed symbols) and site H (open symbols).

tween HCO_3^- concentrations and the saturation index for siderite ($r = 0.71$, $n = 8$) as well as dissolved Fe and $SI_{siderite}$ (r = 0.95, n = 9). Siderite was detected in the XRD-measurements, and geochemical modelling shows that it is strongly supersaturated throughout the profile ($SI_{siderite} = 1.5 \pm 0.3$) (Fig. 6b). This suggests siderite precipitation, despite reported slow kinetics at low temperatures (Postma, 1982). Dissolved Fe concentrations also correlate well with P concentrations (r = 0.84, n = 8), suggesting that phosphate originally adsorbed onto Fe oxide minerals may be released during the dissolution of these phases at site H. The result is that groundwater at site H is also supersaturated with respect to vivianite ($SI_{vivianite} = 1.95 \pm 0.5$) (Fig. 6b). Vivianite was detected in the sediment by XRD, especially in the upper part of the profile.

The hydrochemistry of groundwater at the depth of the gravel layer is broadly similar at both sites (Fig. 5). This holds for dissolved As (~7 μg/L) as well as dissolved Fe (2 mg/L) and P_{tot} (0.3–0.6 mg/L). The deepest groundwater at both sites is supersaturated with respect to calcite and dolomite, as in the shallower sandy aquifer at site L. The concentration of dissolved S is significantly higher in the gravel layer at site L compared to site H, however. The overall patterns suggest that the composition of groundwater at depth in Van Phuc may rather be controlled by region-wide flow through the Pleistocene gravel layer than by differing local conditions.

4.3. Mineralogical and geochemical composition

The bulk mineralogical composition of the sediment at site L and H is very similar. The dominant minerals are quartz (A: 56 ± 19, B: 59 ± 15 wt.%), mica (19 ± 5, 17 ± 8 wt.%), feldspars (10 ± 6, 14 ± 6 wt.%) and kaolinite (7 ± 2, 5 ± 3 wt.%). Variations in their relative proportions with depth depend primarily on grain size. In clayey silt, quartz (44 ± 12, 40 ± 7 wt.%) and feldspars (5 ± 1, 5 ± 1 wt.%) are less abundant, whereas in sand their contribution is significantly higher (quartz: 74 ± 11, 65 ± 11 wt.%; feldspars: 14 ± 4, 15 ± 4 wt.%). The increase is mainly at the expense of phyllosilicates like mica, chlorite, and kaolinite, which are much less abundant in the sandy layers. The contribution of calcite and dolomite is low to undetectable throughout the profiles and could be quantified only in clayey silt (~1 wt.%). Fe minerals such as hematite, goethite, and hornblende are present throughout at site L and in most intervals at site H but their amounts could not be quantified. Minerals such as siderite, ilmenite, vivianite, gibbsite and boehmite were detectable in some but not all intervals at both sites. In the upper portion of site L, pyrite was detected in some samples.

The concentration of As in the solid phase at both sites is within the typical range reported for unconsolidated sediments (Smedley and Kinniburgh, 2002). Concentrations of 1–30 mg/kg As (Fig. 3) are also comparable to previous observations in alluvial systems in Bangladesh or West Bengal where groundwater As levels are also elevated (e.g. Nickson et al., 2000; Swartz et al., 2004; Polizzotto et al., 2006). The concentration of solid As in the sandy deposits is low at both sites with ~5 mg/kg on average, compared to higher values in the upper silty layers of 14.5 ± 7 mg/kg (Fig. 3). Concentrations of As in the solid phase correlate with the silt content ($r_s = 0.81$, $n = 42$) at site L. No such relationship is observed at site H.

Concentrations of Fe in the solid phase (~5 wt.%) are higher in the upper part of the profile at both sites compared to the underlying sandy aquifer (2 wt.%, Fig. 3). Throughout the entire core from site L, there is also a clear relationship between As and Fe concentrations in the solid phase ($r_s = 0.74$, $n = 42$). The relationship is weaker at site H ($r_s = 0.62$, $n = 55$). The molar Fe/As ratio in the solid phase is slightly higher in the aquifer at site L (4000 ± 1500) compared to site H (3200 ± 2000). The ratio is within the range of 4200–4600 previously reported by Berg et al. (2008) for sediments in contact with groundwater high in As in the region.

At both sites organic rich layers were found in the upper part of the profile (Fig. 3). The TOC content is up to 4.5 wt.% at site L but only up to 0.8 wt.% at site H. On average, the concentration of TOC in the sandy deposits is below 0.03 wt.% at both sites. These values are in the same range as previous TOC measurements for aquifers in the Hanoi region of 0.04–0.74 wt.% and 0.02–2.5 wt.% by Postma et al. (2007) and Berg et al. (2008), respectively.

4.4. Sequential extractions

4.4.1. Site L

In the sediment, As appears to be associated with different phases in the upper silty layer and in aquifer sands at site L. In the silty sediment (A8120, A1410, Fig. 2), more than 40% of As was released by phosphate-extraction (F2, Table 2), a fraction associated with strong adsorption. The HCl-extractable fraction is another important pool in this interval (F3, 10–20%) and may represent other host phases such as Mn-oxides, very amorphous Fe-oxides, siderite, vivianite and amorphous Al-oxides. A molar Fe:Al ratio of 9:1 and the low quantities of Mn released in the HCl-treatment compared to Fe and Al suggest that only Fe phases contribute significantly. Additionally, the extractions indicate that sulphides and organic matter (F7) may also contain significant levels of As (20–30%), which would be consistent with elevated total S (TS) (0.2–0.6 wt.%) and TOC (0.7–4 wt.%) concentrations in the upper layer. Compared to fractions F2, F3, and F7, other extractions did not release significant quantities of As from silty sediment at site L (Table 2). Iron was mainly released in the HCl-, HF- and HNO_3/H_2O_2-extraction steps (F3–F6–F7). Possible Fe phases released by these extractions include very amorphous Fe-oxides (i.e., ferrihydrite), siderite, phyllosilicates (i.e., chlorite and biotite), amphiboles and Fe sulfides (e.g. pyrite). Extraction F3 may also include adsorbed Fe(II) (Dixit and Hering, 2006).

In aquifer sands from site L, instead, little As was released by the phosphate extraction whereas more than 90% of As was released by HCl (F3: 35–54%) and DCB (F5: 25–65%, Table 2). The lack of correlation between Fe and As released in F3 and F5 suggests non-Fe containing phases may be significant hosts of As in aquifer sands at site L. These may include amorphous Al-oxides, as suggested by similar Fe and Al concentrations in F3 (3:2). All the other extractions released minor or undetectable levels of As

Table 2
Average partitioning of Fe and As in each fraction of the sequential extraction for all samples from site L and H

	Core L				Core H	
	Silt		Sand			
	As (%)	Fe (%)	As (%)	Fe (%)	As (%)	Fe (%)
F1 (SO_4-step)	4	2	4	<1	5	<1
F2 (PO_4-step)	44	8	<1	3	56	8
F3 (HCl-step)	17	20	46	14	16	16
F4 (Ox-step)	2	4	<1	5	6	8
F5 (DCB-step)	7	6	38	35	6	32
F6 (HCl-step)	1	38	9	41	9	37
F7 (HNO_3/H_2O_2-step)	25	22	2	<1	2	<1
	As (mg/kg)	Fe (g/kg)	As (mg/kg)	Fe (g/kg)	As (mg/kg)	Fe (g/kg)
Total amount in sediments (average)	41	23	2	19	8	23

(Table 2). Most of the Fe present in aquifer sands at site L was released by DCB (13–48%) or HF (26–54%), suggesting the dominance of crystalline Fe-oxides like hematite or goethite, as well as Fe-containing silicates (Table 2).

4.4.2. Site H

In contrast to site L, strongly adsorbed As liberated by the phosphate extraction was by far the dominant pool (F2: >50%) throughout the sandy aquifer at site H (Table 2). Additional quantities of As were also extracted by HCl (F3: 10–20%) and HF (F6: ~9%) solutions. The average molar Fe:Al ratio of 5:2 in the solid phase suggests that amorphous Al-oxides are probably less important at site H than at site L. Contributions of As from other extractions were minor.

At site H, concentrations of Fe in the sediment extractable with DCB and HF are roughly balanced (32–37%) and larger than in the HCl-extractable pool (16%, Table 2). These observations indicate that Fe is mainly bound in crystalline phases like oxides and silicates (hematite, biotite, hornblende, etc.) as well as amorphous phases. Some Fe is also released by the phosphate extraction (~ 8%), indicating that Fe(II) might also be adsorbed to mineral surfaces, and by the oxalate-extraction (~ 8%).

5. Discussion

5.1. Association of arsenic in the sediment

The main difference in sediment geochemistry between the two sites is the extent of reduction of Fe oxhydroxides which, as inferred from colour and reflectance, is much more pronounced in all but the deepest sandy interval at site H compared to site L. In Bangladesh, ΔR values ranging from <0.1 to ~1 correspond to leachable Fe(II)/Fe ratios ranging from >0.9 to ~0.1, respectively (Horneman et al., 2004). There are no other significant mineralogical differences between the two sites, as previously reported elsewhere for aquifers associated with contrasting levels of As in groundwater (Pal et al., 2002; van Geen et al., 2008a). The presence of crystalline Fe(III) oxides like hematite inferred from the sequential extractions is consistent with the brown colour and reflectance of aquifer sands at site L ($\Delta R > 0.7$) (Fig. 3a). The sequential extractions indicate that most of the As in the sediment is associated with these crystalline Fe(III) oxides at site L (Table 2) and, based on the dissolved As profiles, is relatively insoluble. Similar associations have previously been reported for deeper Pleistocene aquifers of Bangladesh (BGS/DPHE, 2001; Harvey et al., 2002; Swartz et al., 2004; Zheng et al., 2005; Stollenwerk et al., 2007).

In contrast, amorphous Fe phases of mixed Fe(II/III) valence are indicated by the grey colour and low ΔR values (<0.25) of aquifer sands at site H (Fig. 3b). The sequential extraction data indicate that As is primarily adsorbed to these phases (Table 2) and, arguably for that reason, also elevated in groundwater (Zheng et al., 2005; van Geen et al., 2006; van Geen et al., 2008a). Elevated Fe(II)/Fe ratios and high concentrations of P-extractable As in grey aquifer sands measured at several nearby locations (van Geen et al., 2008b, 2008a) indicate that conditions at site H are representative of the larger area within Van Phuc where groundwater As concentrations are elevated. The high proportion of adsorbed As in reducing sands is consistent with previous observations by Berg et al. (2008) in this and other areas of Vietnam based on a simplified version of the extraction scheme of Keon et al. (2001). Postma et al. (2007) concluded from their analysis of aquifer sediment from a shallow grey aquifer near the Red River associated with elevated dissolved As that, rather than being adsorbed, As in the solid phase is primarily bound within the lattice of Fe-oxides. The step in their extraction scheme used to identify adsorbed As relies on a 10-fold lower P concentration (Wenzel et al., 2001), which may explain the different attribution.

5.2. Factors contributing to arsenic release and retention

Whereas contrasting redox conditions between sandy aquifers at the two sites are likely to play a role, there is no simple correlation at site H between As and other constituents of groundwater indicative of microbially induced Fe-oxide reduction such as dissolved Fe, NH_4^+ or HCO_3^-. One potential confounding factor is competitive adsorption of As with PO_4^{3-} (Su and Pulse, 2001; Dixit and Hering, 2003; Radu et al., 2005) and HCO_3^-. Dissolved P concentrations are at least an order of magnitude higher at site H compared to site L, and HCO_3^- levels up to threefold higher (Fig. 5). The sequential extraction data show that very little As is adsorbed at site L, however, suggesting that other factors control the release of As to groundwater at this location. There is no clear correlation between dissolved As and P levels even within the profile at site H. Whereas HCO_3^- levels are also generally higher at site H than at site L, the influence of HCO_3^- on the adsorption of As remains unclear Apello et al. (2002) and Anawar et al. (2004) concluded from their experiments that high concentrations of HCO_3^- result in considerable desorption of As. Meng et al. (2000) as well as Radu et al. (2005) could not confirm these results in their studies, however.

The precipitation of secondary mineral phases may be another reason why processes that are likely to influence the partitioning of As between groundwater and aquifer particles are difficult to separate. Several studies have pointed out that siderite can adsorb As or co-precipitate with As (Anawar et al., 2004; Sengupta et al., 2004; Guo et al., 2007). Siderite as well as vivianite are both supersaturated at site H and therefore likely to precipitate (Fig. 6). The reflectance data suggest the formation of amorphous Fe(II)–As(III)-phases at site H and these may have a relatively low affinity for As (Swartz et al., 2004; Horneman et al., 2004; van Geen et al., 2004; Herbel and Fendorf, 2006; Pedersen et al., 2006; Dixit and Hering, 2006; Coker et al., 2006). Dixit and Hering (2006) provided evidence that sorption of As(III) on Fe-minerals is enhanced at higher Fe(II) concentrations, which is the case between 20 and 35 m at site H (Fig. 5), leading to surface-precipitation of Fe(II)–As(III)-bearing phases. On the other hand, the formation of sulphide phases suggested by low dissolved S levels in portions of the aquifer at both sites could result in the loss of As from groundwater (Lowers et al., 2007).

5.3. *Source of organic matter resulting in reducing conditions*

The geochemistry of the sediment and groundwater at sites H and L shows that both aquifers are reducing, although to a different extent. This raises the question of the origin of this contrast in redox conditions. The concentration of NH_4^+, a good indicator of the intensity of NOM degradation (Postma et al., 2007), is much higher at site H (<34 mg/L) compared to site L (<1 mg/L). The depth profiles, therefore, suggest a higher NOM-accessibility at site H compared to site L that is consistent with a more advanced state of reduction. The TOC content of sandy intervals at both sites is comparable and fairly low (L: 0.03 wt.%; H: 0.02 wt.%), which means that the nature of the organic matter would have to be different to account for the observed contrast.

An alternative explanation is that the reactive organic matter reaching sandy aquifers originates primarily from intercalated confining layers (Chapelle and Bradley, 1996; McMahon, 2001). Peat layers have been documented in the Hanoi area and seem to be a common feature (Berg et al., 2001, 2008; Tanabe et al., 2003). The upper layer at site L contains intervals elevated in TOC (Fig. 3a), but concentrations are lower on average compared to site H (0.15 vs. 0.29 wt.%, respectively). At site L, however, this NOM is embedded within a thick silt layer and sealed from the underlying aquifer by Fe concretion. Combined with low NH_4^+ concentrations even in the shallowest well at site L, this suggests little downward transport of the NOM contained in the upper silt layer at site L. At site H instead, the NOM-rich layers are separated from the aquifer by only thin silt lenses and NH_4^+, HCO_3^-, P_{tot} and DOC concentrations are all elevated in the shallowest portion of the aquifer (Fig. 5). The contrast in redox conditions between sites H and L could therefore plausibly be related to enhanced downward transport of organic matter from the top silt layer at site H which is in accordance with the interpretation of Berg et al. (2008). Further study will be required to confirm such a link. The penetration of bomb-produced ^3H in the sandy aquifers at site H and the absence of ^3H at site L (unpublished data, F. Frei and R. Kipfer) might be another indication of a greater supply of reactive organic matter to those aquifers of Van Phuc that are elevated in As.

6. Conclusions

The data presented in this paper show that the sharp contrast in dissolved As concentrations between two portions of a single village on the banks of the Red River cannot be explained by major differences in bulk geochemistry or mineralogy of the sediment. Even if total concentrations of As in sandy parts of the sediment at both sites are comparable, the form and availability of As in aquifer particles is markedly different. At site H, concentrations of dissolved As in groundwater are elevated and As in the solid phase is primarily adsorbed to grey sands of mixed Fe(II/III) valence. The lithology and hydrochemistry of this site suggest that the strongly reducing nature of the aquifers at site H is related to a considerable supply of reactive NOM to the upper portion of the aquifer. At site L instead, As is not adsorbed but more tightly bound mostly within orange-brown Fe(III) oxides. Less reducing conditions at site L inferred from sediment colour and reflectance are consistent with a limited supply of reactive NOM to this location indicated by low levels of Fe, NH_4^+, HCO_3^- and DOC in groundwater compared to site H. Extensive reduction of Fe oxhydroxides in the solid phase appears to be a key step for the release of As to groundwater in Vietnam, although the importance of other contributing factors, such as hydrogeology and the quality of NOM, has yet to be resolved.

Acknowledgements

We acknowledge our colleagues from the Institute for Mineralogy and Geochemistry for analytical support: Utz Kramar (XRF), Beate Oetzel (XRD) and Claudia Mössner (ICP-MS). A special thank to Caroline Stengel who analysed the groundwater samples at Eawag, Switzerland. We are also very grateful to the colleagues at CETASD and HUMG, in particular Tran Nghi, Do Minh Duc, Vi Mai Lan, Dao Manh Phu, Bui Hong Nhat and Pham Qui Nhan for their assistance during the field campaign and the villagers and authorities of Van Phuc for their hospitality. Thanks also to Felix Frei, Zahid Aziz, Kathleen A. Radloff, and Hun-Bok Jung for their participation in the field campaign. For financial support we thank the International Bureau of the German Ministry of Education and Research (BMBF) and the LGK-BW. US-based involvement was funded by NSF Grant EAR 0345688.

References

Anawar, H.M., Akai, J., Sakugawa, H., 2004. Mobilization of arsenic from subsurface sediments by effect of bicarbonate ions in groundwater. Chemosphere 54, 753–762.

Apello, C.A.J., Van der Weiden, M.J.J., Tournassat, C., Charlet, L., 2002. Surface complexation of ferrous iron and carbonate on ferrihydrite and the mobilization of arsenic. Environ. Sci. Technol. 36, 3096–3103.

Berg, M., Tran, H.C., Nguyen, T.C., Pham, H.V., Schertenleib, R., Giger, W., 2001. Arsenic contamination of groundwater and drinking water in Vietnam: a human health threat. Environ. Sci. Technol. 35, 2621–2626.

Berg, M., Luzi, S., Trang, P.T.K., Viet, P.H., Giger, W., Stüben, D., 2006. Arsenic removal from groundwater by household sand filters – comparative field study, model calculations, and health benefits. Environ. Sci. Technol. 40, 5567–5573.

Berg, M., Stengel, C., Trang, P.T.K., Viet, P.H., Sampson, M.L., Leng, M., Samreth, S., Fredericks, D., 2007. Magnitude of arsenic pollution in the Mekong and Red River Deltas – Cambodia and Vietnam. Sci. Total Environ. 372, 413–425.

Berg, M., Trang, P.T.K., Stengel, C., Buschmann, J., Viet, P.H., Dan, N.V., Giger, W., Stüben, D., 2008. Hydrological and sedimentary controls leading to arsenic contamination of groundwater in the Hanoi area, Vietnam: the impact of iron–arsenic ratios, peat, river bank deposits, and excessive groundwater abstraction. Chem. Geol. 249, 91–112.

Beyer, W., 1964. Zur Bestimmung der Wasserdurchlässigkeit von Kiesen und Sanden aus der Kornverteilungskurve. Wasserwirtschaft-Wassertechnik 14, 165–168.

BGS, DPHE, 2001. Arsenic contamination of groundwater in Bangladesh. In: Kinniburg, D.G., Smedley, P.L. (Eds.), Final Report, BGS Technical Report WC/00/19, vol. 2. British Geological Survey, Keyworth, UK.

Bukau, G., Artinger, R., Geyer, S., Wolf, M., Fritz, P., Kim, J.I., 2000. Groundwater in-situ generation of aquatic humic and fulvic acids and the mineralization of sedimentary organic carbon. Appl. Geochem. 15, 819–832.

Buschmann, J., Berg, M., Stengel, C., Sampson, M.L., 2007. Arsenic and manganese contamination of drinking water resources in Cambodia: coincidence of risk areas with low relief topography. Environ. Sci. Technol. 41, 2146–2152.

Buschmann, J., Berg, M., Stengel, C., Winkel, L., Sampson, M.L., Trang, P.T.K., Viet, P.H., 2008. Contamination of drinking water resources in the Mekong delta floodplains: arsenic and other trace metals pose serious health risks to population. Environ. Int. 34, 756–764.

Chapelle, F.H., Bradley, P.B., 1996. Microbial acetogenesis as a source of organic acids in ancient Atlantic Coastal Plain sediments. Geology 24, 925–928.

Charlet, L., Polya, D.A., 2006. Arsenic in shallow, reducing groundwaters in Southern Asia: an environmental health disaster. Elements 2, 91–96.

Chowdhury, T.R., Basu, G.K., Mandal, B.K., Biswas, B.K., Samanta, G., Chowdhury, U.K., Chanda, C.R., Lodh, D., Roy, S.L., Saha, K.C., Roy, S., Kabir, S., Quamruzzaman, Q., Chakrabort, D., 1999. Arsenic poisoning in the Ganges Delta. Nature 401, 545–546.

Coker, V.S., Gault, A.G., Pearce, C.I., van der Laan, G., Telling, N.D., Charnock, J.M., Polya, D.A., Lloyd, J.R., 2006. XAS and XMCD evidence for species-dependent partitioning of arsenic during microbial reduction of ferrihydrite to magnetite. Environ. Sci. Technol. 40, 7745–7750.

Das, D., Samanta, G., Mandal, B.K., Chowdhury, T.R., Chanda, C.R., Chowdhury, P.P., Basu, G.K., Chakraborti, D., 1996. Arsenic in groundwater in six districts of West-Bengal, India. Environ. Geochem. Health 18, 5–15.

Del Razo, L.M., Arellano, M.A., Cebrián, M.E., 1990. The oxidation states of arsenic in well-water from a chronic arsenicism area of northern Mexico. Environ. Pollut. 64, 143–153.

Dixit, S., Hering, J.G., 2003. Comparison of arsenic(V) and arsenic(III) sorption onto iron oxide minerals: implications for arsenic mobility. Environ. Sci. Technol. 37, 4182–4189.

Dixit, S., Hering, J.G., 2006. Sorption of Fe(II) and As(III) on goethite in single- and dual-sorbate systems. Chem. Geol. 228, 6–15.

Dowling, C.B., Poreda, R.J., Basu, A.R., Peters, S.L., Aggarwal, P.K., 2002. Geochemical study of arsenic release mechanisms in the Bengal Basin groundwater. Water Resour. Res. 38, 1173.

Guo, H., Stüben, D., Berner, Z., 2007. Adsorption of arsenic(III) and arsenic(V) from groundwater using natural siderite as the adsorbent. J. Colloilds Interf. Sci. 315, 47–53.

Harvey, C.F., Swartz, C.H., Badruzzaman, A.B.M., Keon-Blute, N., Yu, W., Ashraf Ali, M., Jay, J., Beckie, R., Niedan, V., Brabander, D., Oates, P.M., Ashfaque, K.N., Islam, S., Hemond, H.F., Ahmed, M.F., 2002. Arsenic mobility and groundwater extraction in Bangladesh. Science 298, 1602–1606.

Herbel, M., Fendorf, S., 2006. Biogeochemical processes controlling the speciation and transport of arsenic within iron coated sand. Chem. Geol. 228, 16–32.

Horneman, A., Van Geen, A., Kent, D.V., Mathe, P.E., Zheng, Y., Dhar, R.K., ÓConnell, S.O., Hoque, M.A., Aziz, Z., Shamsudduha, M., Seddique, A.A., Ahmed, K.M., 2004. Decoupling of As and Fe release to Bangladesh groundwater under reducing conditions. Part I: evidence from sediment profiles. Geochim. Cosmochim. Acta 68, 3459–3473.

Keon, N.E., Swartz, C.H., Brabander, D.J., Harvey, C., Hemond, H.F., 2001. Validation of an arsenic sequential extraction method for evaluating mobility in sediments. Environ. Sci. Technol. 35, 2778–2784.

Larson, F., Nhan, P.Q., Nhan, D.D., Postma, D., Jessen, S., Vietn, P.H., Thao, N.B., Huy, T.D., Hoan, N., Chambon, J., Hoan, N.V., Dang, H.H., Nguyen, H.T., Mai, D.T., 2008. Controlling geological and hydrogeological processes in an arsenic contaminated aquifer on the Red River flood plain, Vietnam. Appl. Geochem. 23 (11), 3099–3115.

Lovley, D.R., 1992. Microbial oxidation of organic matter coupled to the reduction of Fe(III) and Mn(IV) oxides. Catena Suppl. 21, 101–114.

Lovley, D.R., Chapelle, F.H., 1995. Deep subsurface microbial processes. Rev. Geophys. 33, 365–381.

Lowers, H.A., Breit, G.N., Foster, A.L., Whitney, J., Yount, J., Uddin, M.N., Muneem, A.A., 2007. Arsenic incorporation into authigenic pyrite, Bengal Basin sediment, Bangladesh. Geochim. Cosmochim. Acta 71, 2699–2717.

Mathers, S., Zalasiewicz, J., 1999. Holocene sedimentary architecture of the Red River Delta, Vietnam. J. Coast. Res. 15, 314–325.

McAthur, J.M., Ravenscroft, P., Safiullah, S., Thirlwall, M.F., 2001. Arsenic in groundwater: testing pollution mechanisms for sedimentary aquifers in Bangladesh. Water Resour. Res. 37, 109–117.

McAthur, J.M., Banerjee, D.M., Hudson-Edwards, K.A., Mishra, R., Purohit, R., Ravencroft, P., Cronin, A., Howarh, R.J., Chatterjee, A., Talukder, T., Lowry, D., Houghton, S., Chadha, D.K., 2004. Natural organic matter in sedimentary basins and its relation to arsenic in anoxic ground water: the examples of West Bengal and its worldwide implications. Appl. Geochem. 19, 1255–1293.

McMahon, P.B., 2001. Aquifer/aquitard interfaces: mixing zones that enhance biogeochemical reactions. Hydrogeol. J. 9, 34–43.

Meng, X., Bang, S., Korfiatis, G.P., 2000. Effects of silicate, sulfate and carbonate on arsenic removal by ferric chloride. Water Res. 34, 1255–1261.

Meng, X., Korfiatis, G.P., Christodoulatos, C., Bang, S., 2001. Treatment of arsenic in Bangladesh well water using a household co-precipitation and filtration system. Water Res. 35, 2805–2810.

Nickson, R.T., McArthur, J.M., Ravenscroft, P., Burgess, W.G., Ahmed, K.M., 2000. Mechanisms of arsenic release to groundwater, Bangladesh and West Bengal. Appl. Geochem. 15, 403–413.

Nicolli, H.B., Suriano, J.M., Peral, M.A.G., Ferpozzi, L.H., Baleani, O.A., 1989. Groundwater contamination with arsenic and other trace-elements in an area of the Pampa, province of Córdoba, Argentina. Environ. Geol. Water Sci. 14, 3–6.

Pal, T., Mukherjee, P.K., Sengupte, S., 2002. Nature of arsenic pollutants in groundwater of Bengal Delta – a case study from Baruipur area, West Bengal, India. Curr. Sci. 82, 554–561.

Parkhurst, D.L., Appelo, C.A., 1999. Useŕs guide to PHREEQC (version 2) – a computer program for speciation, reaction-path, 1D-transport, and inverse geochemical calculations. US Geol. Surv. Water Resour. Invest. Rep., pp. 99–4259.

Pedersen, H.D., Postma, D., Jakobsen, R., 2006. Release of arsenic associated with the reduction and transformation of iron oxides. Geochim. Cosmochim. Acta 70, 4116–4129.

Polizzotto, M.L., Harvey, C.F., Li, G., Badruzzman, B., Ali, A., Newville, M., Sutton, S., Fendorf, S., 2006. Solid-phases and desorption processes of arsenic within Bangladesh sediments. Chem. Geol. 228, 97–111.

Polya, D.A., Gault, A.G., Diebe, N., Feldmann, P., Rosenboom, J.W., Gilligan, E., Fredericks, D., Milton, A.H., Sampson, M., Rowland, H.A.L., Lythgoe, P.R., Jones, J.C., Middleton, C., Cooke, D.A., 2005. Arsenic hazard in shallow Cambodian groundwaters. Mineral. Mag. 69, 807–823.

Postma, D., 1982. Pyrite and siderite formation in brackish and freshwater swamp sediments. Am. J. Sci. 282, 1151–1183.

Postma, D., Larsen, F., Hue, N.T.M., Duc, M.T., Viet, P.H., Nhan, P.Q., Jessen, S., 2007. Arsenic in groundwater of the Red River floodplain, Vietnam: controlling geochemical processes and reactive transport modelling. Geochim. Cosmochim. Acta 71, 5054–5071.

Radu, T., Subacz, J.L., Phillippi, J.M., Barnett, M.O., 2005. Effects of dissolved carbonate on arsenic adsorption and mobility. Environ. Sci. Technol. 39, 7875–7882.

Rowland, H.A.L., Polya, D.A., Lloyd, J.R., Pancost, R.D., 2006. Characterisation of organic matter in a shallow, reducing, arsenic-rich aquifer, West Bengal. Org. Geochem. 37, 1101–1114.

Rowland, H.A.L., Pederick, R.L., Polya, D.A., Pancost, R.A., van Dongen, B.E., Gault, A.G., Bryant, C., Anderson, B., Charnock, J.M., Vaughan, D.J., Lloyd, J.R., 2007. Control of organic matter type of microbially mediated release of arsenic from contrasting shallow aquifer sediments from Cambodia. Geobiology 5, 281–292.

Rowland, H.A.L., Gault, A.G., Lythgoe, P., Polya, D.A., 2008. Geochemistry of aquifer sediments and arsenic-rich groundwaters from Kandal Province, Cambodia. Appl. Geochem. 23 (11), 3029–3046.

Sengupta, S., Mukherjee, P.-K., Pal, T., Shome, S., 2004. Nature and origin of arsenic carriers in shallow aquifer sediments of Bengal Delta, India. Environ. Geol. 45, 1071–1081.

Smedley, P.L., Kinniburgh, D.G., 2002. A review of the source, behaviour and distribution of arsenic in natural waters. Appl. Geochem. 17, 517–568.

Snyder, R.L., Bish, D.L., 1989. Quantitative analysis. In: Bish, D.L., Post, J.E. (Eds.), Modern Powder Diffraction. Reviews in Mineralogy, vol. 20. Mineralogical Society of America, pp. 101–144.

Stollenwerk, K.G., Breit, G.N., Welch, A.H., Yount, J.C., Whitney, J.W., Foster, A.L., Uddin, M.N., Majumder, R.K., Ahmed, N., 2007. Arsenic attenuation by oxidized aquifer sediments in Bangladesh. Sci. Total Environ. 379, 133–150.

Stüben, D., Berner, Z., Chandrasekharam, D., Karmakar, J., 2003. Arsenic enrichment in groundwater of West Bengal, India: geochemical evidence for mobilization of As under reducing conditions. Appl. Geochem. 18, 1417–1434.

Stute, M., Zheng, Y., Schlosser, P., Horneman, A., Dhar, R.K., Datta, S., Hoque, M.A., Seddique, A.A., Shamsudduha Ahmed, K.M., Van Geen, A., 2007. Hydrological control of As concentrations in Bangladesh groundwater. Water Resour. Res. 43, W09417.

Su, C., Pulse, R.W., 2001. Arsenate and arsenite removal by zerovalent iron: effects of phosphate, silicate, carbonate, borate, sulphate, chromate, molybdate and nitrate, relative to chloride. Environ. Sci. Technol. 35, 4562–4568.

Swartz, C.H., Blute, N.K., Badruzzman, B., Ali, A., Barbander, D., Jay, J., Besancon, J., Islam, S., Hemond, H.F., Harvey, C.D., 2004. Mobility of arsenic in a Bangladesh aquifer: Inferences from geochemical profiles leaching data and mineralogical characterisation. Geochim. Cosmochim. Acta 68, 4539–4557.

Tanabe, S., Hori, K., Saito, Y., Haruyama, S., Vu, V.P., Kitamura, A., 2003. Song Hong (Red River) delta evolution related to millennium-scale Holocene sea-level changes. Quaternary Sci. Rev. 22, 2345–2361.

Tanabe, S., Saito, Y., Vu, Q.L., Hanebuth, T.J.J., Ngo, Q.L., Kitamura, A., 2006. Holocene evolution of the Song Hong (Red River) delta system, northern Vietnam. Sediment. Geol. 187, 29–61.

Trafford, J.M., Lawrence, A.R., Macdonald, D.M.J., Nguyen, V.D., Tran, D.N., Nguyen, T.H., 1996. The effect of urbanisation on groundwater quality beneath the city of Hanoi, Vietnam. BGS Technical Report WC/96/22. British Geological Survey, Keyworth, UK.

Tseng, W.P., Chu, H.M., How, S.W., Fong, J.M., Lin, C.S., Yeh, S., 1968. Prevalence of skin cancer in an endemic area of chronic arsenicism in Taiwan. J. Nat. Cancer Inst. 40, 239–254.

van Geen, A., Zheng, Y., Versteeg, R., Stute, M., Horneman, A., Dhar, R., Steckler, M., Gelman, A., Small, C., Ahsan, H., Graiano, J.H., Hussain, I., Ahmed, K.M., 2003. Spatial variability of arsenic in 6000 tube wells in a 25 km^2 area of Bangladesh. Water Resour. Res. 39, 1140.

van Geen, A., Rose, J., Thoral, S., Garnier, J.M., Zheng, Y., Bottero, J.Y., 2004. Decoupling of As and Fe release to Bangladesh groundwater under reducing conditions. Part II: evidence from sediment incubations.. Geochim. Cosmochim. Acta 68, 3475–3486.

van Geen, A., Zheng, Y., Cheng, Z., Aziz, Z., Horneman, A., Dhar, R.K., Mailloux, B., Stute, M., Weinman, B., Goodbred, S., Seddique, A.A., Hoque, M.A., Ahmed, K.M., 2006. A transect of groundwater and sediment properties in Araihazar, Bangladesh: further evidence of decoupling between As and Fe mobilization. Chem. Geol. 228, 85–96.

van Geen, A., Zheng, Y., Goodbred Jr., S., Horneman, A., Aziz, Z., Cheng, Z., Stute, M., Mailloux, B., Weinman, B., Hoque, M.A., Seddique, A.A., Hossain, M.S., Chowdhury, S.H., Ahmed, K.M., 2008a. Flushing history as a hydrogeological control on the regional distribution of arsenic in shallow groundwater of the Bengal Basin. Environ. Sci. Technol. 42, 2283–2288.

van Geen, A., Radloff, K., Aziz, Z., Cheng, Z., Huq, M.R., Ahmed, K.M., Weinman, B., Goodbred, S., Jung, H.B., Zheng, Y., Berg, M., Trang, P.T.K., Charlet, L., Metral, J., Tisserand, D., Guillot, S., Chakraborty, S., Gajurel, A.P., Upreti, B.N., 2008b. Comparison of arsenic concentrations in simultaneously-collected groundwater and aquifer particles from Bangladesh, India, Vietnam, and Nepal. Appl. Geochem. 23 (11), 3244–3251.

van Herreweghe, S., Swennen, R., Vandecasteele, C., Cappuyns, V., 2003. Solid phase speciation of arsenic by sequential extraction in standard reference materials and industrially contaminated soil samples. Environ. Pollut. 122, 323–342.

Wenzel, W.W., Kirchbaumr, N., Prohaska, T., Stingeder, G., Lombic, E., Adriano, D.C., 2001. Arsenic fractionation in soils using an improved sequential extraction procedure. Anal. Chim. Acta 436, 309–323.

White, D.E., Hem, J.D., Waring, G.A., 1963. Chemical composition of subsurface water. Data of Geochemistry. US Geological Survey.

Winkel, L., Berg, M., Amini, M., Hug, S.J., Johnson, C.A., 2008a. Predicting groundwater arsenic contamination in Southeast Asia from surface parameters. Nature Geosci. 1, 536–542.

Winkel, L., Berg, M., Stengel, C., Rosenberg, T., 2008b. Hydrogeological survey assessing arsenic and other groundwater contaminants in the lowlands of Sumatra, Indonesia. Appl. Geochem. 23 (11), 3019–3028.

Zaldivar, B.J., 1974. Arsenic contamination of drinking water and foodstuffs causing endemic chronic poisoning. Beitr. Pathol. 151, 384–400.

Zheng, Y., Stute, M., van Geen, A., Gavrieli, I., Dhar, R., Simpson, H.R., Schlosser, P., Ahmed, K.M., 2004. Redox control of arsenic mobilization in Bangladesh groundwater. Appl. Geochem. 19, 201–214.

Zheng, Y., van Geen, A., Stute, M., Dhar, R., Mo, Z., Cheng, Z., Horneman, A., Gavrieli, I., Simpson, H.J., Versteeg, R., Steckler, M., Grazioli-Venier, A., Goodbred, S., Shahnewaz, M., Shamsudduha, M., Hoque, M.A., Ahmed, K.M., 2005. Geochemical and hydrogeological contrasts between shallow and deeper aquifers in two villages of Araihazar, Bangladesh: implications for deeper aquifers as drinking water sources. Geochim. Cosmochim. Acta 69, 5203–5218.